NUCLEAR FUSION SUPPLEMENT 1991

PLASMA PHYSICS AND CONTROLLED NUCLEAR FUSION RESEARCH 1990

PROCEEDINGS OF THE
THIRTEENTH INTERNATIONAL CONFERENCE ON PLASMA PHYSICS
AND CONTROLLED NUCLEAR FUSION RESEARCH
HELD BY THE
INTERNATIONAL ATOMIC ENERGY AGENCY
IN WASHINGTON, D.C., 1–6 OCTOBER 1990

In three volumes

VOLUME 2

INTERNATIONAL ATOMIC ENERGY AGENCY
VIENNA, 1991

NOVEL COMPUTATIONAL TECHNIQUES TO PREDICT TRANSPORT IN CONFINEMENT DEVICES, AND APPLICATIONS TO ION TEMPERATURE GRADIENT DRIVEN TURBULENCE*

M. KOTSCHENREUTHER, H.L. BERK, R. DENTON, S. HAMAGUCHI, W. HORTON, C.-B. KIM, M. LEBRUN, P. LYSTER, S. MAHAJAN, W.H. MINER, P.J. MORRISON, D.W. ROSS, R.D. SYDORA[1], T. TAJIMA, J.B. TAYLOR, P.M. VALANJU, H.V. WONG, S.Y. XIAO, Y.-Z. ZHANG
Institute for Fusion Studies,
University of Texas at Austin,
Austin, Texas,
United States of America

Abstract

NOVEL COMPUTATIONAL TECHNIQUES TO PREDICT TRANSPORT IN CONFINEMENT DEVICES, AND APPLICATIONS TO ION TEMPERATURE GRADIENT DRIVEN TURBULENCE.

The thermal conductivity χ_i is computed for realistic experimental parameters by several different 3-d simulation techniques for ion temperature gradient driven modes in a slab. A widely used fluid model is also simulated. Both the kinetic χ_i magnitudes and the simulation results are inconsistent with the χ_i profiles seen on TFTR and JET. This indicates that the slab branch of ion temperature gradient driven modes cannot explain experimental transport. Fully kinetic calculations of χ_i are made possible using two different, new gyrokinetic simulation techniques which are up to two orders of magnitude faster than earlier gyrokinetic particle simulations. Both give χ_i in rough agreement with mixing length estimates using linear kinetic eigenfunction scales. However, χ_i is an order of magnitude or more *lower* than inferred values on TFTR and JET. Ion Landau damping and gyroaveraging effects are important for experimental parameters. The kinetic χ_i is an order of magnitude lower than the fluid χ_i but the scaling is similar. The fluid simulation χ_i agrees with mixing length estimates from linear fluid eigenfunctions. The differences between the fluid and kinetic χ_i can be explained by the difference in growth rates and scale lengths present in linear theory, which leads to a difference in the mixing length χ_i of about the same size as that found in the simulations. In a separate study, regression analyses are performed to obtain the local χ_i between the $q = 1$ and $q = 2$ surfaces in terms of the local dimensionless parameters present in the gyrokinetic equation. The slab η_i model does not fit the data well.

* Work supported by US Department of Energy contract DE-FG05-80ET-53088.

[1] Department of Physics, University of California, Los Angeles, California, USA.

KINETIC SIMULATION TECHNIQUES

The nonlinear gyrokinetic equation in slab geometry to lowest order in the gryokinetic expansion is

$$\frac{\partial}{\partial t}\delta f\left(\mathbf{x}, v_\perp, v_\parallel\right) + \hat{z} \times \underline{\nabla}(\phi) \cdot \underline{\nabla}\delta f + v_\parallel \nabla_\parallel \delta f$$

$$= v_\parallel \nabla_\parallel \langle\phi\rangle F_M + \left[1 + \eta\left(v^2 - \frac{3}{2}\right)\right] \underline{\hat{z}} \cdot \underline{\nabla} \langle\phi\rangle \cdot \hat{x} F_M,$$

where $\delta f = h + \langle q\varphi/T_i\rangle f_M$, time is normalized by $\omega_{*_n}^{-1}$, x and y by ρ_i, and $s = L_n/L_s$, and $\langle\ \rangle$ is the gyroaverage. Two totally different algorithms are presented.

a) δf Particle Algorithm. Previous particle algorithms compute the charge density by accumulating the number of particles in a cell. (Gyroaverage effects will be neglected in this discussion for simplicity.) Statistical fluctuations in the number of particles per cell leads to noise in φ, which can swamp the part of φ from saturated instabilities.

In the δf particle algorithm, the nonlinear equation Eq. (1) is solved for δf by integrating S along the nonlinear particle orbits (i.e., the method of characteristics). The particle positions are evolved and act as markers for the value of δf. Note δf is related to the full distribution function f and background distribution f_M by $\delta f = \langle f\rangle - f_M + (\langle\langle q\varphi/T_i\rangle\rangle - q\varphi/T_i) f_M$; thus δf is proportional to the fluctuation amplitude, *not* the background distribution function. The perturbed charge density is computed by accumulating δf on the markers to a grid. Since the nonlinear orbit equations preserve phase space volume, no net marker bunching errors arise. Statistical fluctuations in φ are smaller than previous codes by roughly the factor $\delta f/f$. Typically $\delta f/f \sim 10^{-2}$; the δf algorithm requires orders of magnitude fewer particles to simulate such microinstabilities because of the reduced noise. (Dimitz and Lee independently invented a similar gyrokinetic algorithm, but did not notice the low noise feature.) Note that for 3-d runs, δf was damped to zero near the boundary to prevent quasilinear flattening.

b) Spectral Code. Here, δf is expanded in basis functions: Fourier modes in y and Hermite functions in x, and a grid is used in $v_\parallel$ and $v_\perp$. Large time steps are possible since the linear terms in the equation are solved implicitly, using analytically derived linear orbit integrals over the source term for given φ. Further economies accrue since Hermite functions are close to the linear eigenfunctions, so few are needed.

Boundary conditions in x are chosen so that the energy flux out of one side is put in on the other side, thus preventing profile flattening.

The spectral code is expensive for many modes, so 3-d runs use fewer modes than the δf particle code.

c) Tests and Comparisons. Both codes agree with linear fully gyrokinetic eigenvalue codes, typically to within several percent.

Comparisons were made with a standard gyrokinetic particle code for the nonlinear saturation of a 2d η_i mode in sheared slab. Parameters typical of TFTR were used: $\eta_i = 4$ and $L_n/L_s = 0.25$. However, the standard code needed a large equilibrium gradient scale ($\rho_i/L_n = 1/40$, much stronger than experiment) to increase the saturated amplitude above the noise.

The standard particle code was run with 300 K and 3000 K particles. The 300 K simulation was noise dominated; it showed no well defined exponentiating phase and had a large φ amplitudes. The 3000 K simulation gave a saturated amplitude which agreed well with the δf and spectral code, but required roughly 50 hours of Cray CPU time. Both the δf and spectral codes agreed, using roughly 10 min of Cray CPU time. The δf code gave converged results with 32 K particles (1 K = 1024).

All codes need an order of magnitude more time for 3-d runs. The δf and spectral codes run for acceptable expense ($\sim$ 4 Cray CPU hours). The cost of standard gyrokinetic algorithms for such low noise levels is many hundreds of hours or more.

FLUID SIMULATIONS

A fluid model used by many authors was simulated in sheared slab geometry. The value of the parallel viscosity and parallel pressure diffusion were chosen to mimic the effects of ion Landau damping as well as possible. Extensive parameter scans were done to arrive at the expression $\chi_i = g\,(\rho_s/L_n)\,(cT_i/eB)\,(\eta - \eta_i)\exp(-\alpha s)$, where $g \approx 1$ and $\alpha \approx 5$.

COMPARISONS OF 3D SIMULATIONS

Figure 1 gives a comparison of linear growth rates and scale lengths ($\Delta x^2 = \int \varphi^2\,dx / \int (d\varphi/dx)^2\,dx$). Over most of the kinetic eigenmodes, $\omega/k_\parallel v_i \sim 1$ and $\Delta x \sim \rho_i$. Thus, for experimental parameters kinetic effects such as Landau damping and gyroaveraging are important. This leads to large differences between the fluid model and the kinetic results. Here $\eta/\eta_{\text{critical}} \sim 2$ for both fluid and kinetic cases. Comparison of results for $\eta/\eta_c \sim 4$ shows similar differences.

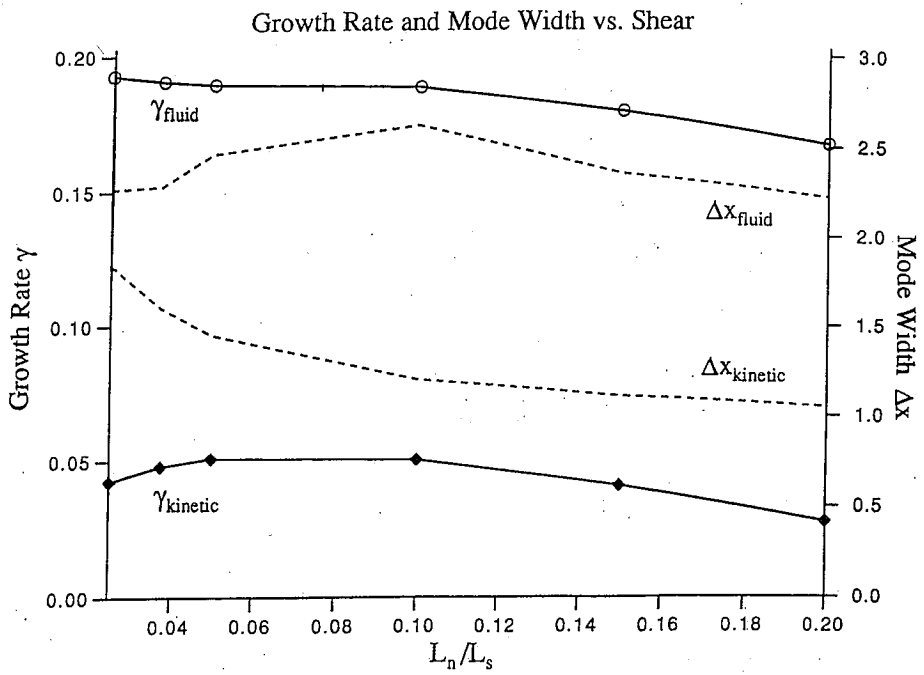

Figure 1. A comparison of the full gyrokinetic model for growth rates and mode widths of η_i modes. Parameters used are η_i=2, $k_y\rho_i$=0.8 and T_i/T_e=1.

The linear mixing length estimates of the fluid and kinetic cases differ by roughly 20. The simulation results for χ_i differ similarly. Results for the normalized heat conductivity F, defined by $\chi_i = (v_i\rho_i^2/L_n)\,F\,(\eta_i, L_s/L_n, T_i/T_e)$, are shown in Fig. 2. Despite the linear discrepancy, one might have hoped that simpler fluid models are closer to more complete kinetic models for nonlinear dynamics. This is not found. Similar results are found for $2 < \eta < 5$.

Also, note that the δf code and the spectral code agree to within a factor of 2. The differences may be attributed to the different number of Fourier modes used in the two codes, the somewhat different boundary conditions in x, and to the presence of small dissipative terms in the spectral code added for numerical reasons.

For both kinetic codes, most of the transport comes from modes with the highest linear growth rates, at $k\rho_i \sim .35 - .7$. The spectrum drops to much smaller values as $k\rho_i$ increases.

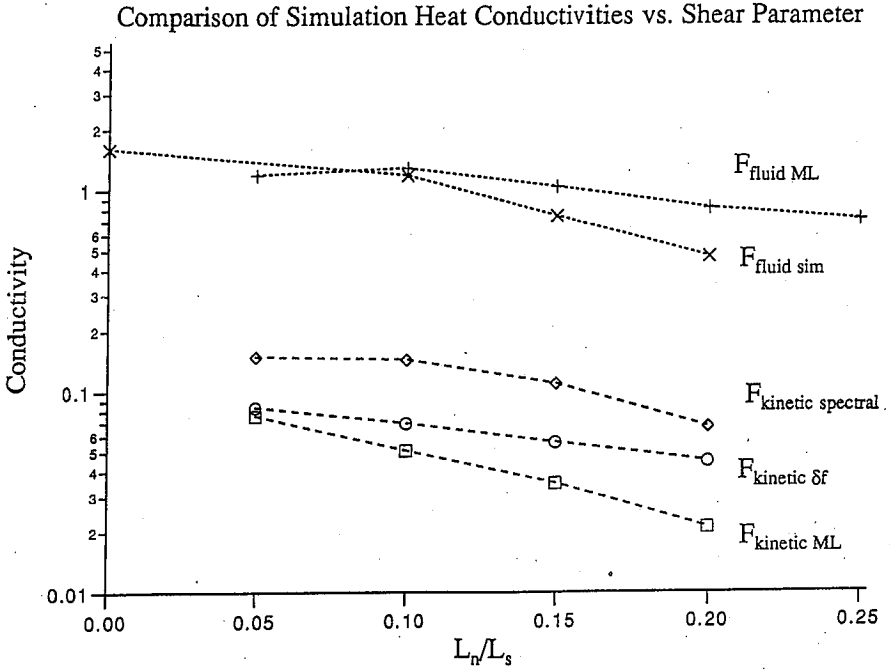

Figure 2. Normalized conductivity F for η_i=2, T_i/T_e=1, computed by fluid simulation ($F_{fluid\ sim}$), fluid eigenfunction mixing length estimate ($F_{fluid\ ML}$), kinetic δf code ($F_{kinetic\ \delta f}$), kinetic spectral code ($F_{kinetic\ spectral}$) and the kinetic eigenfunction mixing length estimate ($F_{kinetic\ ML}$).

In Fig. 3 we compare the kinetic and fluid χ_i with values inferred from experiment. In all cases, the χ_i from slab η_i modes strongly decreases with minor radius, in contradiction with TFTR and JET observations. Also, the kinetic simulation values are much lower than the inferred values. Thus, we conclude that slab η_i modes produce insufficient transport (especially at larger minor radii) to explain the experimental χ_i.

Toroidicity induced η_i modes and trapped particle modes may produce larger transport. Support for this possibility has been found in fully toroidal particle simulations using a code with full Lorentz ion dynamics and drift kinetic electrons. Toroidal runs with $\eta_i = \eta_e = 1$ have been found to have an order of magnitude more transport than otherwise equivalent cylindrical runs. Fluctuations in the saturated state had coupled poloidal harmonics with the same frequency, indicative of a toroidicity induced mode. Further simulations to test these possibilities, including runs with toroidal versions of the spectral code and with the δf particle code, are in progress.

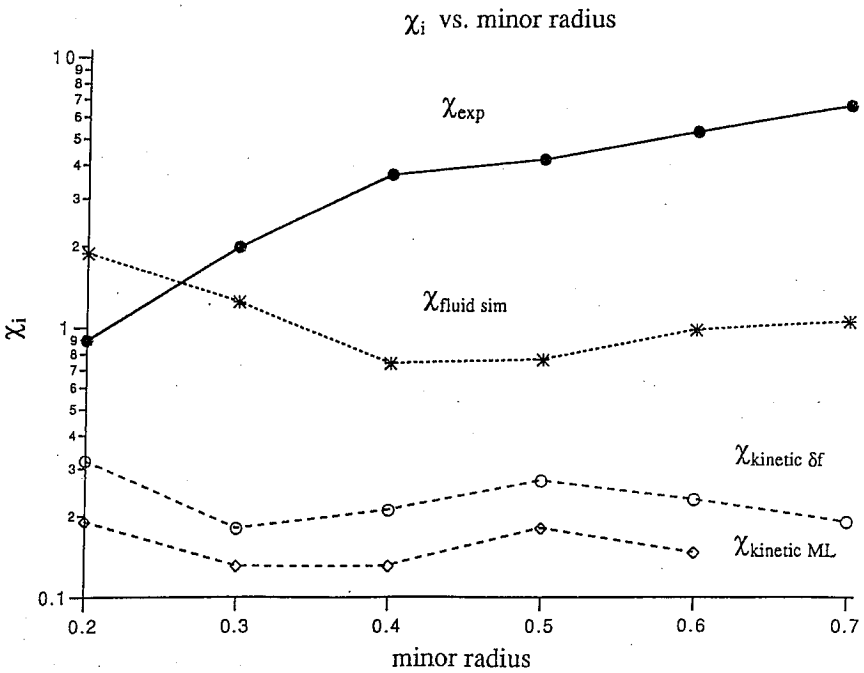

Figure 3. Comparisons of χ_i from experimental data analysis (χ_{exp}), fluid simulation ($\chi_{fluid\ sim}$), the kinetic δf code ($\chi_{kinetic\ \delta f}$), and the kinetic eigenfunction mixing length estimate ($\chi_{kinetic\ ML}$).

We turn now to the statistical analysis of experimental data. Scaling arguments applied to the gyrokinetic equation show that $\chi_i = (v_i\rho_i^2/L_n)\,F\,(\eta_i, L_s/L_n, T_i/T_e)$. Regression was used to obtain the best power law expression for F for beam heated TFTR shots, for minor radii between $q = 1$ and $q = 3$ surfaces, to obtain $F = 0.17\eta_i^{1.0}\,(L_s/L_n)^{.3}\,(T_e/T_i)^{1.4}$. The scaling with η and L_n/L_s is roughly similar to the simulation results. However the best fit did not explain 75% of the variation in the logarithm of χ_i. The experimental data scatter away from the fit value by a factor of 3 both high and low. This poor fit indicates that variables other than those arising in slab η_i modes are needed to reproduce the experimental χ_i.

REFERENCES

[1] HORTON, W., ESTES, R.D., BISKAMP, D., Plasma Phys. **22** (1980) 663.

[2] FREIMAN, E., CHEN, L., Phys. Fluids **25** (1982) 502.

[3] SYDORA, R.D., HAHM, T.S., LEE, W.W., DAWSON, J.M., Phys. Rev. Lett. **64** (1990) 2015.